沉积学报
ACTA SEDIMENTOLOGICA SINICA
ISSN 1000-0550
CN 62-1038/P

中上扬子区上二叠统大隆组硅质岩沉积终结年龄

韦恒叶, 张淦, 张璇, 胡谍, 龚嘉欣

文章编号:1000-0550(2024)06-2135-09　　DOI: 10.14027/j.issn.1000-0550.2024.065

中上扬子区上二叠统大隆组硅质岩沉积终结年龄

韦恒叶[1,2,3],张淦[1,2,3],张璇[1,2,3],胡谍[1,2,3],龚嘉欣[1,2,3]
1.西南石油大学地球科学与技术学院,成都　610500
2.西南石油大学羌塘盆地研究院,成都　610500
3.西南石油大学油气藏地质与开发工程国家重点实验室,成都　610500

摘　要　**【目的】**晚二叠世扬子板块北缘台地内部盆地广旺海槽、开江—梁平海槽与鄂西海槽发育大隆组富有机质的黑色硅质岩沉积,是四川盆地二叠系页岩气勘探的目标层位。这套硅质岩开始沉积于258.77 Ma,其形成与峨眉山地幔柱活动有关,但硅质岩沉积结束的具体年龄以及这些海槽消亡的原因尚不清楚。开展相应的研究有助于深入了解扬子北缘这些深水海槽的演化与发展,为二叠系页岩气勘探潜力评价提供理论依据。**【方法】**采集位于广旺海槽的旺苍燕儿洞剖面上二叠统大隆组硅质岩上部火山灰夹层样品,开展锆石激光剥蚀电感耦合等离子体质谱仪(LA-ICP-MS)分析,测定锆石U-Pb年龄以及微量元素。**【结果】**锆石为自形棱角状,发育生长环带,Th/U≥0.46,球粒陨石标准化的稀土配分曲线展示重稀土富集、轻稀土亏损、Ce正异常、Eu负异常的左倾特征;锆石铀铅年龄为253.0±1.3 Ma;锆石微量元素Th/Nb与Hf/Th交会图以及Th/U与Nb/Hf交会图指示岛弧造山构造背景。**【结论】**华南大隆组硅质岩沉积终结于晚二叠世长兴中期253.0±1.3 Ma,该期火山喷发与板内造山的峨眉山地幔柱活动无关,其形成与扬子板块周围岛弧火山作用有关,后者可能与扬子北缘多个海槽在二叠纪末期萎缩消失密切相关。

关键词　U-Pb定年;岛弧火山;大隆组;晚二叠世;四川盆地;海槽消亡

第一作者简介　韦恒叶,男,1980年出生,博士,教授,博士生导师,沉积学与地球化学,E-mail: hy.wei@swpu.edu.cn

中图分类号　P595　**文献标志码**　A

0　引言

我国华南地区上二叠统上部地层普遍发育一套黑色层状硅质岩(也称为硅岩)沉积,统称为大隆组。在中上扬子区,这套硅质岩形成于台内盆地环境,例如广旺海槽和鄂西海槽等[1-2]。在广旺海槽沉积盆地,由东部的燕儿洞至西部的剑阁上寺,大隆组硅质岩沉积厚度逐渐减薄,在斜坡环境相变为硅质灰岩(图1),盆地环境的沉积厚度约10 m;在鄂西盆地如恩施地区,大隆组硅质岩也具有类似的沉积厚度(图1)。大隆组硅质岩的下部地层为吴家坪组碳酸盐岩,地层过渡段由硅质灰岩突变或渐变为硅质岩,发育密集的火山灰层(图1)。因此,虽然大隆组硅质岩从岩相证据上指示为放射虫、硅质海绵等生物成因[5-8],但地球化学信号反映硅具有生物、热液以及火山喷发物质的混合来源[7,9-10]。这些热液和火山作用与峨眉山地幔柱(亦称峨眉地裂)活动、特提斯洋裂离以以及秦岭勉略洋的裂陷有关[5,11],说明吴家坪浅水台地沉积之后形成的大隆组台内盆地硅质岩沉积是在伸展构造背景下形成的断陷盆地[12],是东吴运动在中上扬子区的伸展裂陷作用产物[11]。大隆组硅质岩沉积的结束时间指示中上扬子区东吴运动裂陷活动的结束时代,尽管大隆组硅质岩开始沉积的年龄已经明确(258.77±0.67 Ma[4]),但目前仍缺乏相应的绝对年龄的约束。因此,选择广旺海槽的旺苍燕儿洞剖面大隆组硅质岩的火山灰夹层斑脱岩为研究对象,开展锆石LA-ICP-MS U-Pb年龄分析,研究大隆组硅质岩沉积结束的年龄,约束大隆组富有机质黑色岩系的沉积年龄,为华南二叠系页岩气勘探提供依据。

1　地质背景

晚二叠世早期,扬子区发生东吴运动,在我国西南地区喷发了大量的玄武岩,构成了峨眉山大火成

收稿日期:2024-02-26;**修回日期:**2024-05-09;**录用日期:**2024-06-08;**网络出版日期:**2024-06-08
基金项目:国家自然科学基金项目(42272118);四川省自然科学基金项目(2023NSFSC0279)[**Foundation**: National Natural Science Foundation of China, No. 42272118; Natural Science Foundation of Sichuan Province, No. 2023NSFSC0279]

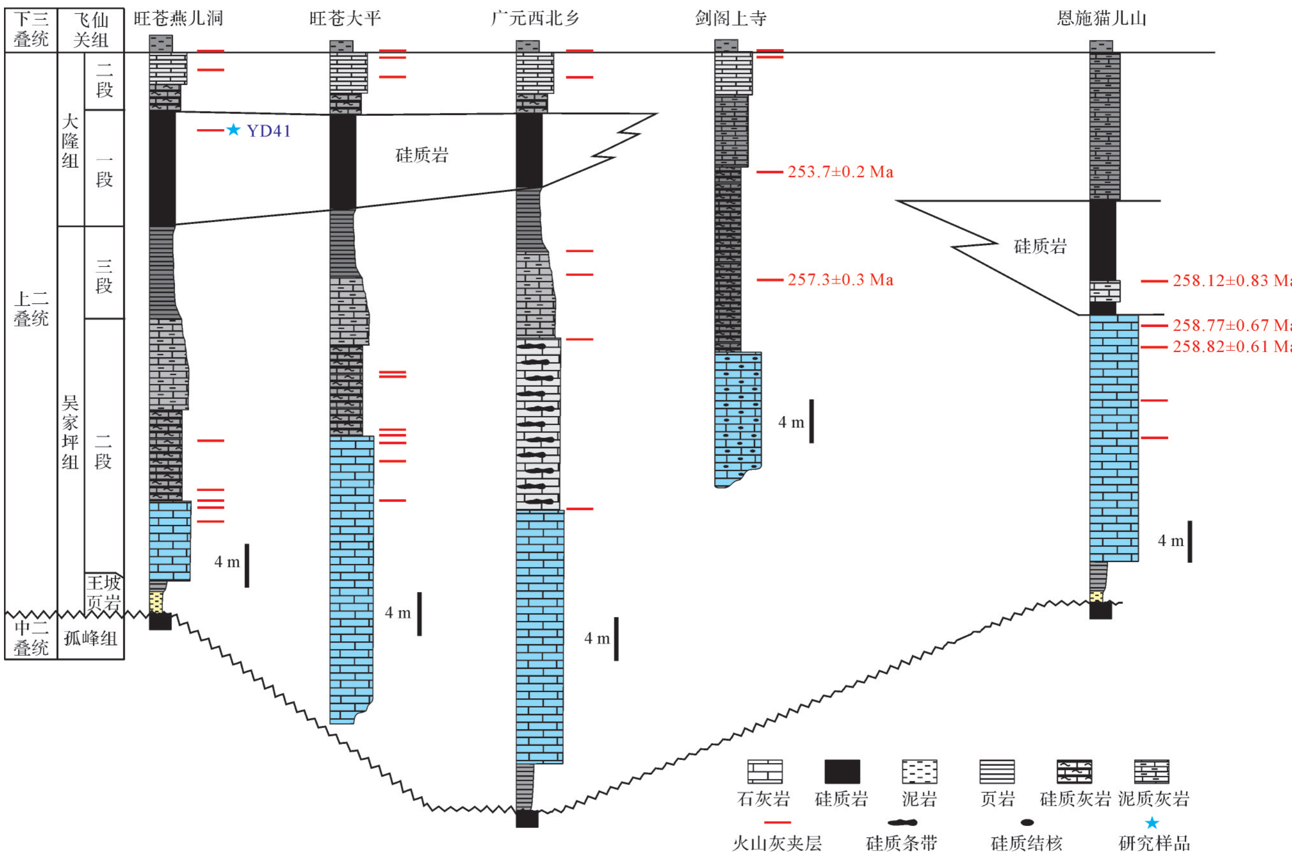

图1 华南上二叠统大隆组地层格架

地层段划分根据文献[1],剑阁上寺剖面和恩施猫儿山剖面锆石U-Pb年龄分别来自文献[3]和文献[4]

Fig.1 Stratigraphic framework in the Dalong Formation in Upper Permian, South China

Member subdivision is from reference [1]; Zircon U-Pb ages of the Shangsi section in Jiange and of the Maoershan section in Enshi are from references [3] and [4] respectively

岩省。峨眉山溢流玄武岩的分布西至理塘,东至桂西,南至越北,北至川东北达州(图2a),分布面积为0.25×10^6 km^2,体积为0.5×10^6 km^3[14-15,17]。近年来,四川盆地油气勘探发现在开江、梁平以及忠县一带的DY-1、FT1等钻井在中—上二叠统界线钻遇玄武岩[16,18],同时在广元西北乡野外剖面的茅口组一段发育辉绿岩岩墙侵入体。峨眉山溢流玄武岩已被证实与地幔柱活动有关,称为峨眉山地幔柱[15,19-21]。地幔柱隆升活动过程包括地幔岩浆上涌、到达并撞击岩石圈底部、地壳抬升、火山喷发、地壳沉降等五个过程[22]。地幔柱头部到达岩石圈之后,发生侧向扩张延展,由原来的400 km直径拓展2倍至800~1 000 km,分别对应着内带和中带的范围[23]。在峨眉山大火成岩省主喷发之前和之后分别发育了中二叠统孤峰组和上二叠统大隆组硅质岩沉积。

由于东吴运动,华南晚二叠世时期古地理发生了根本性的变化,在原来中二叠世巨型碳酸盐岩台地基础上形成了隆凹格局的古地理面貌(图2b)。在西昌—攀枝花—昆明一带形成南北向的康滇古陆,古陆周围向外分布带状的海陆过渡相、浅海碳酸盐岩台地相和深水盆地相,总体展示穹状隆起的古地理特征[23-24]。位于外带的深水盆地相沉积了大隆组黑色硅质岩,例如位于川北的广元至梁平的广旺—开江梁平海槽以及湖北西部的鄂西海槽发育大量的富有机质硅质岩夹页岩。该套页岩和硅质岩目前是四川盆地及其周缘二叠系页岩气勘探目的层,近年来更是取得了突破性的进展,获得了可观的工业气流,是非常规油气勘探的新层位和新领域[25-26]。

2 样品与实验方法

在燕儿洞剖面采集大隆组上部硅质岩夹层中斑脱岩样品约1 kg(图3)。斑脱岩夹层为黄白色,夹于黑色页岩和黑色硅质岩之间,遇水黏手。该类斑脱岩在大隆组黑色硅质岩和页岩中发育多层,本次选

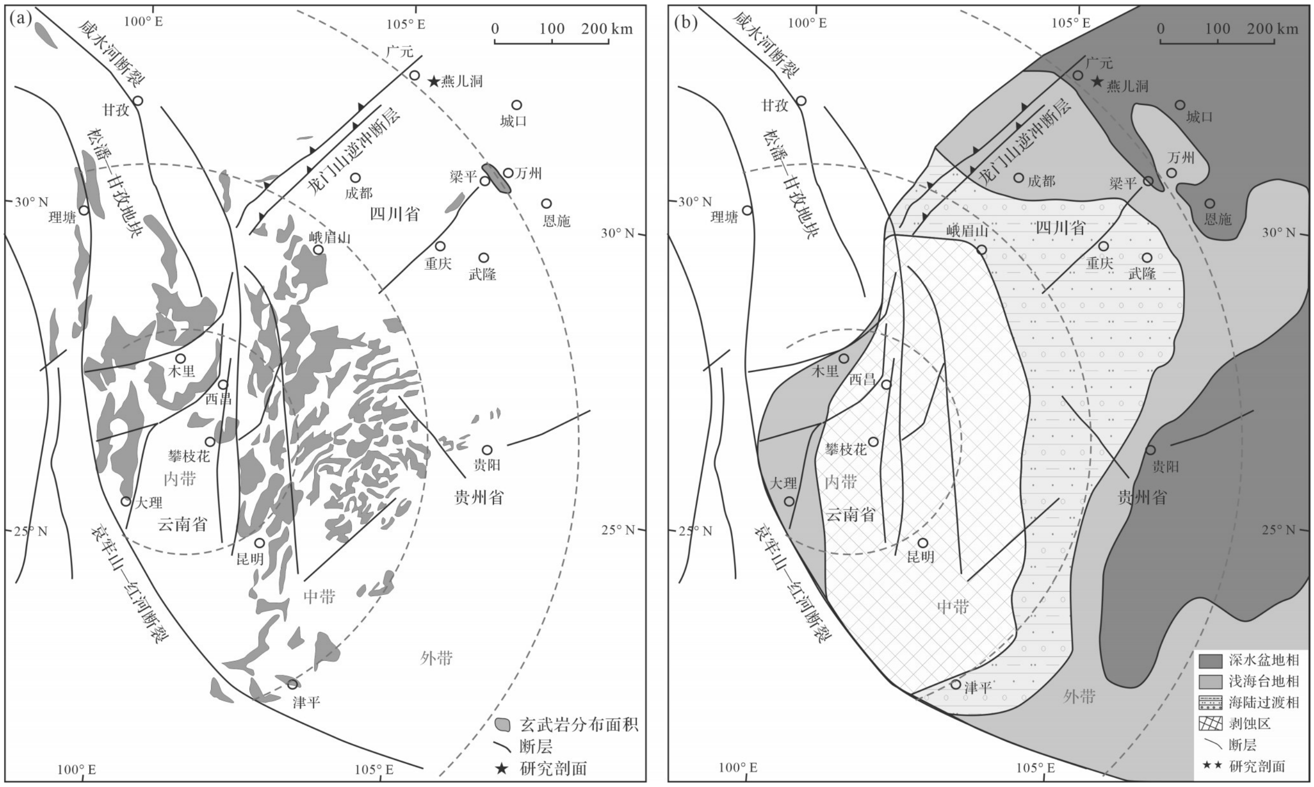

图2　研究区区域地质背景图

(a)峨眉山大火成岩省溢流玄武岩分布特征(据文献[13-16]修改);(b)西南地区晚二叠世古地理特征(据文献[24]修改)

Fig.2　Maps of geological setting in the study area

(a) basalt distribution in the Emeishan large igneous province (modified from references [13-16]); (b) Late Permian paleogeography in southwestern China (modified from reference [24])

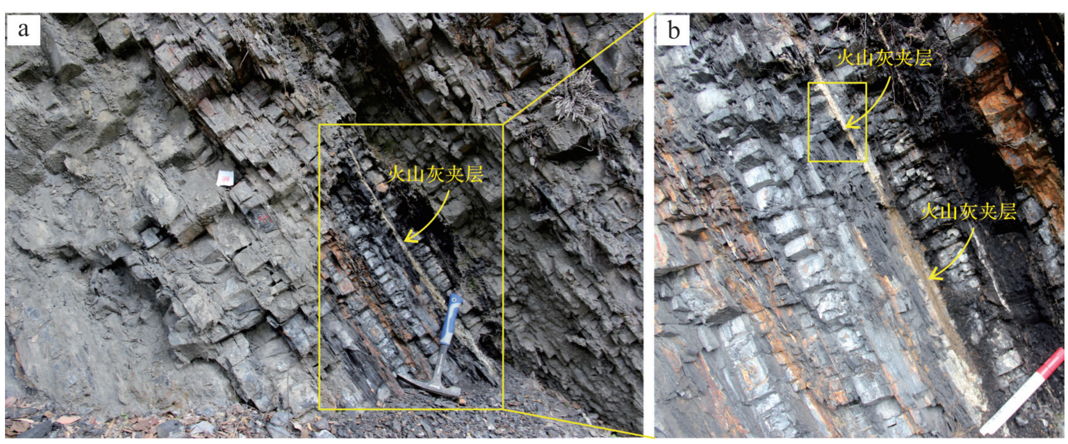

图3　斑脱岩(火山灰)夹层野外特征

Fig.3　Bentonite (volcanic ash) bed intercalated by black chert beds

择大隆组硅质岩段顶部的斑脱岩夹层作为研究对象(图1)。样品烘干后,采用传统锆石分选方法,经过磁选和重液分选后在双目镜下挑选晶形规则、颗粒较大的锆石。将挑选好的锆石切割并抛光以便露出锆石内部结构,用环氧树脂包埋固定,在扫描电子显微镜以及光学显微镜下进行观察并拍照阴极发光和透反射相片。锆石原位U-Pb年龄的测定采用激光剥蚀电感耦合等离子体质谱(Laser Ablation Inductively Coupled Plasma mass Spectrometry,LA-ICP-MS)技术,在武汉上谱分析公司实验室完成。激光剥蚀系统为COMPexPro 102 ArF 193 nm准分子激光剥蚀系统(GeoLas HD),ICP-MS型号为Agilent 7900,激光束斑和频率分别为32 μm和5 Hz,锆石U-Pb同位素定年和微量元素含量处理采用锆石标准91500和玻璃标

准物质NIST610作外标进行同位素和微量元素分馏校正。

3 结果与讨论

3.1 锆石年龄

斑脱岩样品中含丰富的锆石颗粒，用于铀铅LA-ICP-MS测年的锆石颗粒为自形棱角状，发育清楚的震荡生长环带，是典型的岩浆锆石（图4）。样品测定了17个数据点，测定的锆石年龄与同位素比值见表1。锆石中Th和U的含量一般较高，分析样品的U介于（236~479）×10^{-6}，平均值为337×10^{-6}，Th含量介于（109~305）×10^{-6}，平均值为184×10^{-6}，Th/U比值介于0.46~0.64，平均值为0.54，均大于0.46，同样指示岩浆成因性质[27]，这是因为岩浆锆石的Th/U比一般大于或等于0.5[28]。锆石分析点的$^{206}Pb/^{238}U$年龄介于249~258 Ma，加权平均年龄为253.0±1.3 Ma（95%置信度，MSWD=1.12）（图5），代表了火山喷发时棱角状锆石结晶年龄。由于该样品火山灰夹层正好位于大隆组硅质岩段的顶部，因此，大隆组硅质岩沉积的结束年龄约为253.0±1.3 Ma，属于长兴期中期年龄，晚于广元上寺剖面硅质灰岩上部年龄253.7 Ma[3]，代表大隆组硅质岩终结年龄，也意味着二叠纪—三叠纪过渡期“硅质岩缺口”的开始。

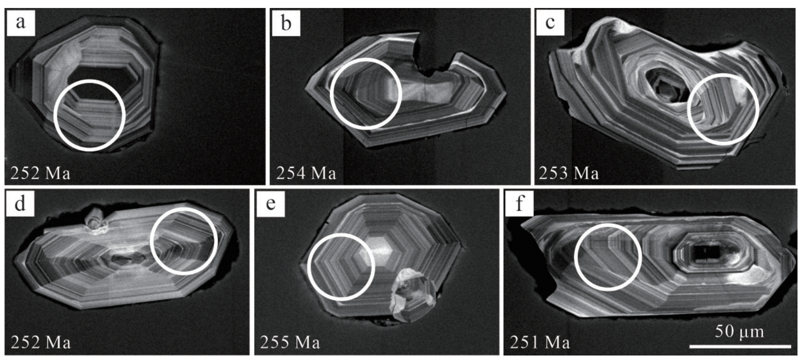

图4 四川旺苍燕儿洞剖面大隆组上部斑脱岩锆石阴极发光图

Fig.4 Cathodoluminescence images of zircons from bentonite layers in the Dalong Formation in the Yan′erdong section, Wangcang, Sichuan province

表1 四川旺苍燕儿洞剖面大隆组斑脱岩锆石同位素比值和年龄测定结果

Table 1 Isotopic ratios and age dating data of zircon in the bentonite in the Dalong Formation in the Yan´erdong section, Wangcang, Sichuan province

样品号	Pb/×10^{-6}	Th/×10^{-6}	U/×10^{-6}	Th/U	Pb/×10^{-6}	$^{207}Pb/^{235}U$	1σ	$^{206}Pb/^{238}U$	1σ	($^{207}Pb/^{206}Pb$)/Ma	1σ	($^{207}Pb/^{235}U$)/Ma	1σ	($^{206}Pb/^{238}U$)/Ma	1σ
YD41-2-01	15.05	174	305	0.57	0	0.296 6	0.011	0.039 9	0.000 5	361	81	264	8	252	3
YD41-2-02	11.20	109	237	0.46	0	0.276 9	0.013	0.039 7	0.000 5	220	101	248	10	251	3
YD41-2-10	11.72	124	236	0.53	0.13	0.284 0	0.011	0.040 6	0.000 6	254	88	254	9	256	4
YD41-2-11	17.38	180	353	0.51	0.46	0.266 3	0.010	0.040 3	0.000 4	106	89	240	8	255	3
YD41-2-13	13.04	137	270	0.51	0.06	0.277 9	0.011	0.039 8	0.000 4	217	94	249	9	252	3
YD41-2-17	15.11	146	308	0.47	0	0.282 2	0.011	0.040 3	0.000 5	220	91	252	9	255	3
YD41-2-19	19.76	223	404	0.55	0	0.298 8	0.010	0.040 4	0.000 5	345	78	265	8	255	3
YD41-2-20	22.94	305	479	0.64	0	0.269 0	0.009	0.039 1	0.000 5	176	76	242	7	247	3
YD41-2-21	17.45	204	356	0.57	0.57	0.285 2	0.010	0.039 8	0.000 4	276	88	255	8	251	2
YD41-2-23	15.89	177	326	0.54	0	0.286 8	0.009	0.040 5	0.000 4	261	84	256	7	256	3
YD41-2-24	16.20	186	330	0.57	0.40	0.281 9	0.012	0.040 1	0.000 5	217	100	252	10	254	3
YD41-2-25	16.42	186	330	0.56	0	0.288 5	0.012	0.040 8	0.000 5	250	94	257	9	258	3
YD41-2-26	13.50	135	279	0.48	0.21	0.297 1	0.012	0.040 0	0.000 4	369	94	264	9	253	3
YD41-2-27	21.22	267	430	0.62	0.28	0.280 3	0.010	0.039 8	0.000 4	220	74	251	8	252	3
YD41-2-28	13.41	132	277	0.48	0	0.278 8	0.011	0.040 9	0.000 5	176	131	250	9	258	3
YD41-2-32	22.75	267	473	0.56	0.01	0.281 7	0.010	0.039 4	0.000 4	280	85	252	8	249	2
YD41-2-33	16.75	180	343	0.52	0.33	0.279 6	0.009	0.039 9	0.000 4	228	78	250	7	252	2

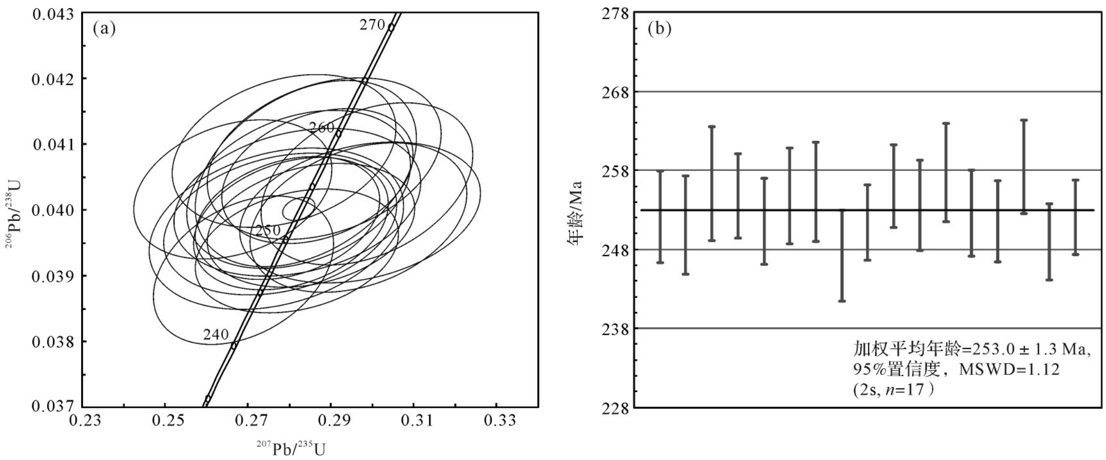

图5　四川旺苍燕儿洞剖面大隆组上部斑脱岩锆石LA-ICP-MS U-Pb定年谐和图(a)和年龄加权平均直方图(b)

Fig.5　(a) LA-ICP-MS U-Pb dating concordia diagram, and (b) individual ages of zircon analyses from bentonite layers in the Dalong Formation in the Yan′erdong section, Wangcang, Sichuan province

3.2　锆石微量元素指示的构造背景

锆石稀土元素(Rare Earth Element, REE)总量∑REE介于$(626\sim985)\times10^{-6}$, Hf含量介于$(8\ 032\sim9\ 170)\times10^{-6}$(表2)。锆石稀土元素球粒陨石标准化的配分模式反映重稀土富集、轻稀土亏损、Ce的正异常以及Eu的负异常的特征,轻稀土一般小于100倍的球粒陨石值,重稀土一般大于10 000倍的球粒陨石值,总体表现为从轻稀土向重稀土逐渐爬升的左倾曲线趋势,(图6),这是未发生蚀变的岩浆锆石的特征[27]。锆石Ce正异常说明锆石是在氧化条件下结晶的,这与样品为喷发火山灰性质一致,而Eu的负异常可能是锆石结晶过程中或结晶之前长石从岩浆中分馏导致岩浆Eu的亏损所致[29]。

锆石的微量元素能够反映岩浆母源组成并指示岩浆宿主的构造背景特征[30-31]。Hf离子半径与Zr相似,因而锆石中含丰富的Hf,样品锆石Hf含量介于$(8\ 032\sim9\ 170)\times10^{-6}$,平均值达$8\ 472\times10^{-6}$(表2)。样品锆石中Nb含量很低,介于$(1.31\sim3.42)\times10^{-6}$,平均为$2.30\times10^{-6}$,与大陆岛弧和洋中脊来源的锆石Nb含量相似,而不同于板内背景下岩浆锆石较高的Nb含

表2　四川旺苍燕儿洞剖面大隆组斑脱岩锆石微量元素含量($\times10^{-6}$)

Table 2　Zircon trace element data in the bentonite in the Dalong Formation in the Yan′erdong section, Wangcang, Sichuan province ($\times10^{-6}$)

样品号	La	Ce	Pr	Nd	Sm	Eu	Gd	Tb	Dy	Ho	Er	Tm	Yb	Lu	Ti	Nb	Hf	Ta
YD41-2-01	0.003 1	9.57	0.026	0.83	2.21	0.46	14.5	5.13	72.2	30.9	156	35.0	334	75.0	3.35	2.27	8 222	0.95
YD41-2-02	0.053 0	8.10	0.031	0.60	1.40	0.20	11.7	4.22	59.2	25.6	130	29.5	289	66.3	2.61	1.97	9 170	1.09
YD41-2-10	0.003 0	6.88	0.053	1.07	3.01	0.62	18.0	6.86	90.2	37.6	182	40.2	386	85.1	3.45	1.31	8 032	0.63
YD41-2-11	0.009 0	9.43	0.060	1.16	2.13	0.45	15.5	5.83	82.2	35.4	182	41.2	410	93.5	4.10	2.56	8 524	1.17
YD41-2-13	0.013 0	8.25	0.063	0.91	2.82	0.60	18.6	7.32	97.0	40.7	202	44.5	432	95.9	4.71	2.06	8 075	0.90
YD41-2-17	0.003 1	8.85	0.041	0.91	1.96	0.61	15.1	5.75	83.8	35.5	181	41.3	414	94.5	4.10	2.67	8 064	1.15
YD41-2-19	0.003 3	11.00	0.031	0.79	1.86	0.49	15.0	5.72	77.8	34.8	175	39.6	390	89.1	2.96	2.64	8 889	1.31
YD41-2-20	0.027 0	12.60	0.086	1.69	2.97	0.42	18.3	6.91	94.4	40.4	201	45.6	446	100.0	3.10	3.42	8 476	1.52
YD41-2-21	0.001 0	10.30	0.058	1.35	2.69	0.66	19.4	7.26	97.9	42.0	208	46.1	450	99.2	2.94	2.59	8 203	0.98
YD41-2-23	0.005 7	8.67	0.027	0.81	2.24	0.44	13.2	4.95	69.1	29.0	143	31.5	304	67.2	3.52	1.88	8 379	0.91
YD41-2-24	20.300 0	54.30	5.570	27.10	6.86	0.86	18.1	5.82	75.3	31.2	152	33.2	323	70.8	4.10	1.95	8 305	0.96
YD41-2-25	0	9.84	0.042	0.66	1.72	0.39	13.9	5.34	71.1	31.0	149	32.9	317	70.0	4.41	1.99	8 601	0.91
YD41-2-26	0.003 1	9.30	0.066	1.09	3.03	0.58	17.9	6.88	94.1	40.8	204	46.3	456	102.0	5.44	2.40	8 083	0.95
YD41-2-27	0.003 2	11.10	0.060	0.97	2.27	0.44	16.1	6.28	81.8	34.3	169	37.5	355	77.7	3.61	2.09	8 537	1.12
YD41-2-28	0.006 3	8.12	0.040	0.80	1.78	0.42	14.1	5.26	71.1	31.6	159	36.1	360	81.3	4.13	2.25	8 372	0.99
YD41-2-32	0.009 0	11.70	0.052	0.64	1.91	0.40	15.8	5.95	79.5	35.8	178	41.2	407	92.2	2.16	3.01	9 135	1.42
YD41-2-33	0.006 1	9.27	0.083	1.24	2.95	0.52	19.1	7.40	96.9	40.8	201	45.4	442	98.7	2.54	2.04	8 955	1.14

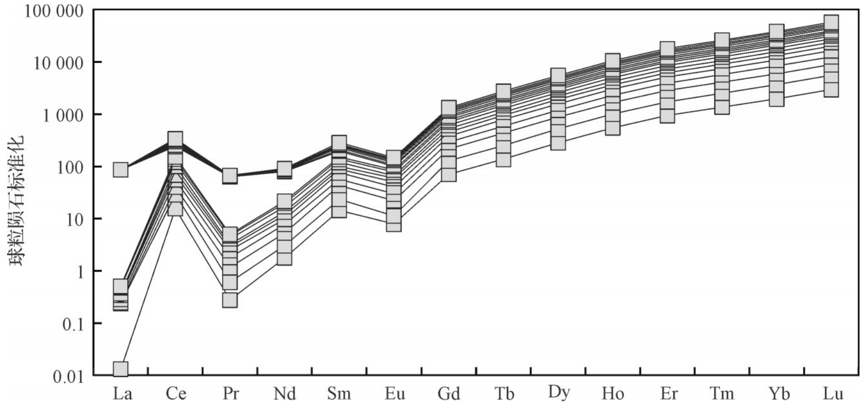

图6 四川旺苍燕儿洞剖面大隆组上部斑脱岩锆石的球粒陨石标准化稀土元素配分模式图

Fig.6 Chondrite-normalized REE patterns of zircon from bentonite layers in the Dalong Formation in the Yan′erdong section, Wangcang, Sichuan province

量[32-33]。Nb一般与岩浆熔融过程中的不相容元素Th为正相关关系，岛弧锆石的Th/Nb比值一般大于10，而板内和洋中脊锆石Th/Nb比值一般小于20[31]，同时岛弧岩浆比板内岩浆锆石具有更低的Nb/Hf和更高的Th/U比值[34-35]。由于富Th矿物优先结晶，岛弧岩浆锆石具有低Th/Nb和高Hf/Th比值的特征[35-37]，因此可以利用这些参数来识别锆石岩浆母源的构造背景。Th/Nb与Hf/Th交会图以及Th/U与Nb/Hf交会图中，燕儿洞剖面大隆组顶部和上部火山灰锆石样品落在岛弧岩浆范围内，而不是落在板内造山范围(图7)。其他地区上二叠统吴家坪组以及大隆组的火山灰锆石构造背景的分析也表明[4,38]：湖北西部以及四川剑阁上寺吴家坪阶的火山灰锆石性质为板内造山背景，与峨眉山大火成岩省关系密切[4]，而长兴阶的火山灰锆石性质却为岛弧性质。这表明广元旺苍县燕儿洞大隆组沉积晚期的火山喷发可能是周围岛弧性质火山喷发所致，属于汇聚型板块边界的岩浆岛弧性质[38]，而不是板内性质峨眉山地幔柱活动的结果。

3.3 大隆组硅质岩年龄的意义

四川盆地广旺海槽及其周缘鄂西盆地大隆组硅质岩含多层火山灰夹层，大隆组下部吴家坪阶的硅质岩内火山灰夹层锆石指示板内造山性质[4]，说明该期火山喷发与板内造山性质的峨眉山大火成岩省(或地幔柱)活动有关。地幔柱形成过程中，地壳抬

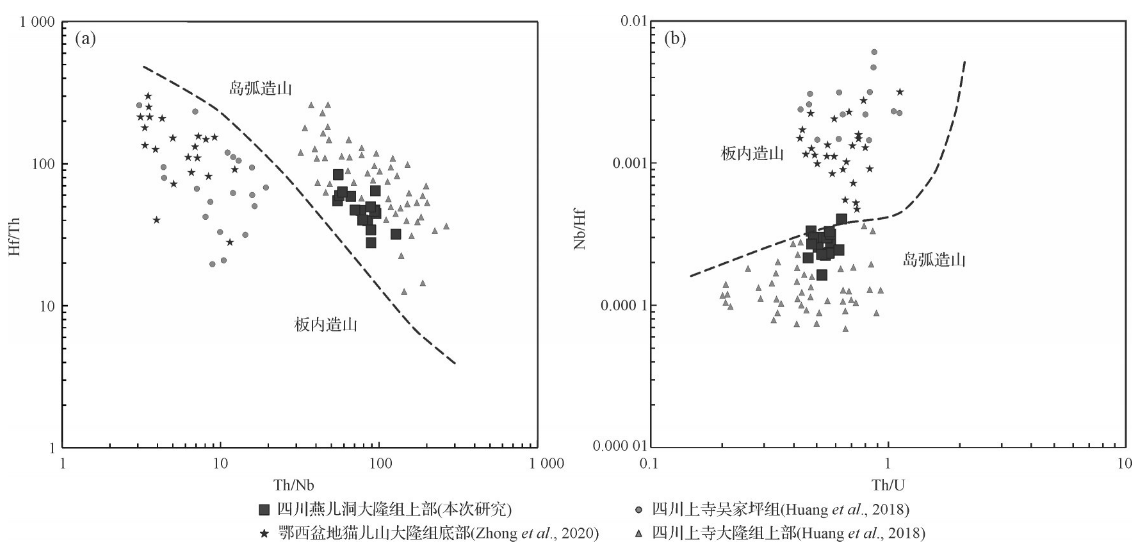

图7 四川旺苍燕儿洞剖面大隆组斑脱岩夹层锆石微量元素构造背景交会图

(a)Th/Nb vs. Hf/Th以及(b)Th/U vs Nb/Hf交会图；底图据文献[4,34]修改

Fig.6 Tectonic setting crossplots for zircons from bentonite in the Dalong Formation in the Yan′erdong section, Wangcang, Sichuan province

(a) Th/Nb vs. Hf/Th; (b) Th/U vs. Nb/Hf; Diagram is modified from references [4,34]

升之后发生裂谷或地堑地垒式台内盆地[22,39],诱发海底活跃的热液活动[40]。峨眉山大火成岩省(地幔柱)中心位于攀枝花地区,地幔柱头部在到达岩石圈之前约400 km,碰撞岩石圈底部之后侧向扩展为800~1 000 km,也即峨眉山大火成岩省中带与外带的分界面[17,41]。而广旺海槽以及鄂西海槽位于外带边缘(图1),远离峨眉山地幔柱头部岩浆的影响范围。但是,近年来四川盆地油气勘探钻井发现,在广旺海槽钻遇大量的峨眉山玄武岩[16,18]以及部分野外辉绿岩岩墙,地幔柱岩浆在侧向上可以通过岩墙和岩石圈底部软流圈进行远距离扩张[42-43]。峨眉山地幔柱岩浆的影响范围可能包括广旺海槽、开江—梁平海槽以及鄂西海槽的外带。峨眉山大火成岩省(地幔柱)在中—晚二叠世过渡期大规模喷发之后,可能形成多个裂谷性质(地堑地垒)断陷盆地或海槽,海底频繁的热液活动以及陆地喷发的玄武岩风化带来的硅质在海洋较深水盆地中富集形成大隆组硅质岩。

然而,大隆组上部和顶部长兴阶硅质岩内火山灰夹层锆石与二叠纪末期火山灰锆石一样,属于岛弧造山构造背景[4,38],说明大隆组沉积晚期火山喷发与峨眉山大火成岩省活动无关,而与扬子板块周围的岛弧火山的活动有关[43]。推测长兴期扬子板块北部出现明显的岩浆岛弧活动,该活动可能与大隆组硅质岩盆地环境萎缩灭亡密切相关。

4 结论

四川盆地广旺海槽上二叠统大隆组硅质岩上部火山灰夹层锆石的铀铅LA-ICP-MS测年表明,大隆组硅质岩沉积结束于253.0±1.3 Ma,属于长兴期中期。锆石稀土元素展示重稀土富集、轻稀土亏损、Ce正异常和Eu负异常的左倾配分曲线特征,痕量元素Th/U比绝大部分大于0.5,指示岩浆锆石的特征。锆石Th/Nb与Hf/Th以及Th/U与Nb/Hf交会图反映锆石岩浆母源为岛弧造山构造背景,与二叠纪末期扬子板块周围岩浆岛弧活动有关,而与板内造山成因的峨眉山大火成岩省无关。晚二叠世长兴中期的岛弧火山活动可能与扬子北缘多个海槽在二叠纪末期萎缩消失密切相关。

致谢 感谢两名审稿专家提出的建设性建议,论文成果过程得到了兰中伍研究员以及陶继华副教授的指导,在此致以感谢。

参考文献(References)

[1] 韦恒叶,胡谍,邱振,等. 川北—鄂西上二叠统富有机岩沉积与地球化学特征[J]. 沉积学报,2024,42(3):766-789. [Wei Hengye, Hu Die, Qiu Zhen, et al. Sedimentological and geochemical characteristics of Late Permian organic-rich rocks in north Sichuan and west Hubei provinces[J]. Acta Sedimentologica Sinica, 2024, 42(3): 766-789.]

[2] 邱振,窦立荣,吴建发,等. 川北—鄂西地区中二叠统层序岩相古地理演化及页岩气勘探潜力[J]. 地球科学,2024,49(2):712-748. [Qiu Zhen, Dou Lirong, Wu Jianfa, et al. Lithofacies palaeogeographic evolution of the Middle Permian sequence stratigraphy and its implications for shale gas exploration in the northern Sichuan and western Hubei provinces[J]. Earth Science, 2024, 49 (2): 712-748.]

[3] Mundil R, Ludwig K R, Metcalfe I, et al. Age and timing of the Permian mass extinctions: U/Pb dating of closed-system zircons [J]. Science, 2004, 305(5691): 1760-1763.

[4] Zhong Y T, Mundil R, Chen J, et al. Geochemical, biostratigraphic, and high-resolution geochronological constraints on the waning stage of Emeishan large igneous province[J]. GSA Bulletin, 2020, 132(9/10): 1969-1986.

[5] 朱洪发,秦德余,刘翠章. 论华南孤峰组和大隆组硅质岩成因、分布规律及其构造机制[J]. 石油实验地质,1989,11(4):341-348. [Zhu Hongfa, Qin Deyu, Liu Cuizhang. On the origin, distributive pattern and tectonic control of siliceous rocks in Gufeng and Dalong Formations, South China[J]. Experimental Petroleum Geology, 1989, 11(4): 341-348.]

[6] 雷卞军,阙洪培,胡宁,等. 鄂西古生代硅质岩的地球化学特征及沉积环境[J]. 沉积与特提斯地质,2002,22(2):70-79. [Lei Bianjun, Que Hongpei, Hu Ning, et al. Geochemistry and sedimentary environments of the Palaeozoic siliceous rocks in western Hubei[J]. Sedimentary Geology and Tethyan Geology, 2002, 22(2): 70-79.]

[7] Chen H, Xie X N, Hu C Y, et al. Geochemical characteristics of Late Permian sediments in the Dalong Formation of the Shangsi section, northwest Sichuan Basin in South China: Implications for organic carbon-rich siliceous rocks formation[J]. Journal of Geochemical Exploration, 2012, 112: 35-53.

[8] 方雪,周瑶琪,姚旭,等. 四川广元上寺上二叠统硅质岩地球化学特征及成因分析[J]. 矿物岩石,2017,37(1):93-102. [Fang Xue, Zhou Yaoqi, Yao Xu, et al. Geochemical characteristics and petrogenesis of siliceous rocks from Shangsi section in Guangyuan, Sichuan province[J]. Journal of Mineralogy and Petrology, 2017, 37(1): 93-102.]

[9] 徐跃通. 鄂东南晚二叠世大隆组层状硅质岩成因地球化学及沉积环境[J]. 桂林工学院学报,1997,17(3):204-212. [Xu Yuetong. Genetic geochemistry for the bedded silicalite in the Late Permian Dalong Formation and its sedimentary setting in southeastern Hubei[J]. Journal of Guilin Institute of Technology, 1997,

17(3): 204-212.]

[10] Gao P, Xiao X M, Meng G M, et al. Quartz types and origins of the Upper Permian Dalong Formation shale of the Sichuan Basin: Implications for pore preservation in deep shale reservoirs [J]. Marine and Petroleum Geology, 2023, 156: 106461.

[11] 杜远生,殷鸿福,王治平. 秦岭造山带晚加里东—早海西期的盆地格局与构造演化[J]. 地球科学:中国地质大学学报,1997,22(4):401-405. [Du Yuansheng, Yin Hongfu, Wang Zhiping. The Late Caledonian-Early Hercynian basin's framework and tectonic evolution of Qingling orogenic belt[J]. Earth Science: Journal of China University of Geosciences, 1997, 22(4): 401-405.]

[12] 陈洪德,王成善,刘文均,等. 华南二叠纪层序地层与盆地演化[J]. 沉积学报,1999,17(4):529-535. [Chen Hongde, Wang Chengshan, Liu Wenjun, et al. Permian sequence stratigraphy and basin evolution in south of China[J]. Acta Sedimentologica Sinica, 1999, 17(4): 529-535.]

[13] 梁新权,周云,蒋英,等. 二叠纪东吴运动的沉积响应差异:来自扬子和华夏板块吴家坪组或龙潭组碎屑锆石LA-ICPMS U-Pb年龄研究[J]. 岩石学报,2013,29(10):3592-3606. [Liang Xinquan, Zhou Yun, Jiang Ying, et al. Difference of sedimentary response to Dongwu Movement: Study on LA-ICPMS U-Pb ages of detrital zircons from Upper Permian Wujiaping or Longtan Formation from the Yangtze and Cathaysia Blocks[J]. Acta Petrologica Sinica, 2013, 29(10): 3592-3606.]

[14] He B, Xu Y G, Chung S L, et al. Sedimentary evidence for a rapid, kilometer-scale crustal doming prior to the eruption of the Emeishan flood basalts[J]. Earth and Planetary Science Letters, 2003, 213(3/4): 391-405.

[15] Xu J F, Suzuki K, Xu Y G, et al. Os, Pb, and Nd isotope geochemistry of the Permian Emeishan continental flood basalts: Insights into the source of a large igneous province[J]. Geochimica et Cosmochimica Acta, 2007, 71(8): 2104-2119.

[16] Liu Y D, Li L, van Wijk J, et al. Surface-wave tomography of the Emeishan large igneous province (China): Magma storage system, hidden hotspot track, and its impact on the Capitanian mass extinction[J]. Geology, 2021, 49(9): 1032-1037.

[17] Xu Y G, He B, Chung S L, et al. Geologic, geochemical, and geophysical consequences of plume involvement in the Emeishan flood-basalt province[J]. Geology, 2004, 32(10): 917-920.

[18] Liu X Y, Qiu N S, Søager N, et al. Geochemistry of Late Permian basalts from boreholes in the Sichuan Basin, SW China: Implications for an extension of the Emeishan large igneous province[J]. Chemical Geology, 2022, 588: 120636.

[19] Chung S L, Jahn B M. Plume-lithosphere interaction in generation of the Emeishan flood basalts at the Permian-Triassic boundary[J]. Geology, 1995, 23(10): 889-892.

[20] Thompson G M, Ali J R, Song X Y, et al. Emeishan basalts, SW China: Reappraisal of the formation's type area stratigraphy and a discussion of its significance as a large igneous province[J]. Journal of the Geological Society, 2001, 158(4): 593-599.

[21] Ali J R, Thompson G M, Song X, et al. Emeishan basalts (SW China) and the 'end-Guadalupian' crisis: Magnetobiostratigraphic constraints[J]. Journal of the Geological Society, 2002, 159 (1): 21-29.

[22] Pirajno F. Mantle plumes, associated intraplate tectonomagmatic processes and ore systems[J]. Episodes, 2007, 30(1): 6-19.

[23] He B, Xu Y G, Wang Y M, et al. Sedimentation and lithofacies paleogeography in southwestern China before and after the Emeishan flood volcanism: New insights into surface response to mantle plume activity[J]. The Journal of Geology, 2006, 114(1): 117-132.

[24] Hou Z S, Fan J X, Henderson C M, et al. Dynamic palaeogeographic reconstructions of the Wuchiapingian stage (Lopingian, Late Permian) for the South China Block[J]. Palaeogeography, Palaeoclimatology, Palaeoecology, 2020, 546: 109667.

[25] 胡德高,周林,包汉勇,等. 川东红星地区HY1井二叠系页岩气勘探突破及意义[J]. 石油学报,2023,44(2):241-252. [Hu Degao, Zhou Lin, Bao Hanyong, et al. Breakthrough and significance of Permian shale gas exploration of well HY1 in Hongxing area, eastern Sichuan Basin[J]. Acta Petrolei Sinica, 2023, 44(2): 241-252.]

[26] 杨雨,汪华,谢继容,等. 页岩气勘探新领域:四川盆地开江—梁平海槽二叠系海相页岩气勘探突破及展望[J]. 天然气工业,2023,43(11):19-27. [Yang Yu, Wang Hua, Xie Jirong, et al. Exploration breakthrough and prospect of Permian marine shale gas in the Kaijiang-Liangping trough, Sichuan Basin[J]. Natural Gas Industry, 2023, 43(11): 19-27.]

[27] Hoskin P W O, Schaltegger U. The composition of zircon and igneous and metamorphic petrogenesis[J]. Reviews in Mineralogy and Geochemistry, 2003, 53(1): 27-62.

[28] Ahrens L H. Some observations on the uranium and thorium distributions in accessory zircon from granitic rocks[J]. Geochimica et Cosmochimica Acta, 1965, 29(6): 711-716.

[29] Hoskin P W O. Patterns of chaos: Fractal statistics and the oscillatory chemistry of zircon[J]. Geochimica et Cosmochimica Acta, 2000, 64(11): 1905-1923.

[30] Belousova E, Griffin W, O'Reilly S Y, et al. Igneous zircon: Trace element composition as an indicator of source rock type [J]. Contributions to Mineralogy and Petrology, 2002, 143(5): 602-622.

[31] Grimes C B, Wooden J L, Cheadle M J, et al. "Fingerprinting" tectono-magmatic provenance using trace elements in igneous zircon[J]. Contributions to Mineralogy and Petrology, 2015, 170 (5/6): 46.

[32] Sun S S, McDonough W F. Chemical and isotopic systematics of oceanic basalts: Implications for mantle composition and processes[J]. Geological Society, London, Special Publications, 1989, 42(1): 313-345.

[33] Pearce J A, Peate D W. Tectonic implications of the composition of volcanic arc magmas[J]. Annual Review of Earth and Plane-

tary Sciences, 1995, 23: 251-285.

[34] Hawkesworth C J, Kemp A I S. Using hafnium and oxygen isotopes in zircons to unravel the record of crustal evolution[J]. Chemical Geology, 2006, 226(3/4): 144-162.

[35] Yang J H, Cawood P A, Du Y S, et al. Large igneous province and magmatic arc sourced Permian-Triassic volcanogenic sediments in China[J]. Sedimentary Geology, 2012, 261-262: 120-131.

[36] Hoskin P W O, Kinny P D, Wyborn D, et al. Identifying accessory mineral saturation during differentiation in granitoid magmas: An integrated approach[J]. Journal of Petrology, 2000, 41(9): 1365-1396.

[37] Tani K, Dunkley D J, Kimura J I, et al. Syncollisional rapid granitic magma formation in an arc-arc collision zone: Evidence from the Tanzawa plutonic complex, Japan[J]. Geology, 2010, 38(3): 215-218.

[38] Huang H, Cawood P A, Hou M C, et al. Provenance of Late Permian volcanic ash beds in South China: Implications for the age of Emeishan volcanism and its linkage to climate cooling[J]. Lithos, 2018, 314-315: 293-306.

[39] Pirajno F, Santosh M. Mantle plumes, supercontinents, intracontinental rifting and mineral systems[J]. Precambrian Research, 2015, 259: 243-261.

[40] Falkenberg J J, Keith M, Haase K M, et al. Effects of fluid boiling on Au and volatile element enrichment in submarine arc-related hydrothermal systems[J]. Geochimica et Cosmochimica Acta, 2021, 307: 105-132.

[41] Wilson M. Thermal evolution of the Central Atlantic passive margins: Continental break-up above a Mesozoic super-plume [J]. Journal of the Geological Society, 1997, 154(3): 491-495.

[42] Ernst R E, Buchan K L. Recognizing mantle plumes in the geological record[J]. Annual Review of Earth and Planetary Sciences, 2003, 31: 469-523.

[43] Xie S C, Pancost R D, Wang Y B, et al. Cyanobacterial blooms tied to volcanism during the 5 m. y. Permo-Triassic biotic crisis [J]. Geology, 2010, 38(5): 447-450.

Termination Age of the Chert Deposits in the Late Permian Dalong Formation in Middle and Upper Yangtze Area, China

WEI HengYe[1,2,3], ZHANG Gan[1,2,3], ZHANG Xuan[1,2,3], HU Die[1,2,3], GONG JiaXin[1,2,3]

1. School of Geoscience and Technology, Southwest Petroleum University, Chengdu 610500, China

2. Qiangtang Institute of Sedimentary Basin, Southwest Petroleum University, Chengdu 610500, China

3. State Key Laboratory of Oil and Gas Reservoir Geology and Exploitation, Southwest Petroleum University, Chengdu 610500, China

Abstract: [**Objective**] Several intraplatform deep-marine trough basins in the northern Yangtze Platform developed bedded chert in the Dalong Formation during the Late Permian. The organic-rich black rocks in the trough basins are shale gas exploration targets in the Sichuan Basin. The black chert deposition in the Dalong Formation started at 258.77 Ma, related to waning of the Emeishan mantle plume. However, its termination date and the cause of the disappearance of the intraplatform trough basins were still unclear. The results of this study help to better understand the evolution of these deep-marine troughs, offering a theoretical basis for potential assessment and exploration of Permian shale gas. [**Methods**] Zircon U-Pb LA-ICP-MS age dating and trace element measurement in the bentonite interbeds were carried out in the upper part of the Dalong Formation chert beds. [**Results**] The zircon grains are euhedral and show clear zoning, with Th/U ratios higher than 0.46. The zircon grains are enriched in heavy rare earth elements (HREE) with positive Ce anomalies and negative Eu anomalies, showing a rising trend from light REE to HREE in the chondrite-normalized REE patterns. The U-Pb LA-ICP-MS age of the zircon was 253.0±1.3 Ma. Diagrams of Th/Nb vs. Hf/Th and Th/U vs. Nb/Hf in the zircon show arc magma origin. [**Conclusions**] Chert deposition in the Dalong Formation in South China ceased in the mid-Changhsingian Stage of the Late Permian at 253.0±1.3 Ma. The arc volcanism eruption was not related to intraplate Emeishan mantle plume activity, but was caused by arc activity around the Yangtze Block, and was probably related to the disappearance of the deep-marine troughs in the northern Yangtze area.

Key words: U-Pb dating; arc volcanism; Dalong Formation; Late Permian; Sichuan Basin; trough disappearance